VCU
VIRGINIA COMMONWEALTH UNIVERSITY

Virginia Commonwealth University
VCU Scholars Compass

Chemistry Publications

Dept. of Chemistry

1996

A Monte Carlo study of methanol clusters (CH3OH)N, N=5-256

D. Wright
Virginia Commonwealth University

M. S. El-Shall
Virginia Commonwealth University, mselshal@vcu.edu

Follow this and additional works at: http://scholarscompass.vcu.edu/chem_pubs

Part of the Chemistry Commons

A Monte Carlo study of methanol clusters (CH$_3$OH)$_N$, $N=5-256$

D. Wright and M. S. El-Shall[a]

Department of Chemistry, Virginia Commonwealth University, Richmond, Virginia 23284-2006

The thermodynamic and structural properties of methanol clusters (CH$_3$OH)$_N$, $N=5-15$, 20, 30, 60, 128, 256 and the bulk liquid have been investigated using Monte Carlo simulation. Calculated properties as a function of size include electrostatic and dispersive contributions to the configurational energy, configurational heat capacities, fractal dimension, density profiles, order parameters characterizing dipole and bond vector orientation, and the Lindemann index. The cluster heat capacities as a function of N possess an interior maximum near $N=128$ and converge to the bulk value from above. Monocyclic, semiplanar structures are found to persist at liquidlike temperatures up to about $N=12$, followed by bi- and polycyclic structures for $N=13-20$, with the larger clusters gradually becoming more spherical. The average density of the larger clusters is fairly well represented by the bulk value. For clusters with 30 or more molecules, there is a net tendency for the molecular dipoles to lie flat on the cluster surface. The observed trends in heat capacities, density profiles, and dipole alignments parallel to the cluster surface are likely to be general features of clusters of polar molecules. © *1996 American Institute of Physics.* [S0021-9606(96)51047-0]

I. INTRODUCTION

Hydrogen bonding is one of the most fundamental intermolecular interactions in chemistry and biology. It plays a major role in determining the static and dynamic properties of many important liquids such as water, alcohols, and other protic solvents.[1–3]

While water is the most unusual hydrogen-bonded liquid with a unique characteristic of forming tetrahedral networks, methanol is the smallest alcohol that can interact by both hydrogen bonding and hydrophobic forces.[4] It differs substantially from water in the tendency to form chainlike polymeric units in the liquid similar to those found in the solid state.[5,6] The bulk liquid has been studied by several simulation methods such as Monte Carlo (MC) and molecular dynamics (MD) and for the most part, good agreements with the available experimental data for various structural and dynamic properties have been obtained.[7–19] Nevertheless, many details concerning molecular association and the structures of various H-bonded clusters in liquid methanol still remain unclear. For example, the dominance of small open chains of sequentially H-bonded monomers has been challenged by the assumption of a cyclic planar hexamer which can apparently provide a very good fit to the x-ray diffraction data of liquid methanol.[20]

Valuable insights into the evolution of the bulk properties of methanol and the transition from molecular to macroscopic systems can be obtained by simulation studies of finite size clusters. Such studies to investigate the thermodynamic, structural, and dynamic properties of isolated clusters have attracted much interest in recent years.[20–23] Much of the work has focused on phase transitions and coexistence phenomena mostly in atomic and rare gas clusters.[24–27] In the case of molecular clusters, this inter-

est in melting transitions has included, for example, benzene,[28,29] TeF$_6$,[30] *t*-butyl chloride,[31] carbon dioxide,[32] acetonitrile,[34–36] and water.[37,38] Isolated molecular clusters of hydrogen fluoride,[39] acetonitrile,[34] and carbon dioxide[40] have also been simulated as an aid in interpreting their IR spectra.

Looking at clusters in a different way, there have been studies of clusters in equilibrium with their vapor, either as single liquid drops[40–45] or within a clustering vapor.[46,47] Thompson *et al.*[42] and Schreve *et al.*[41] have performed MD studies of systems of Lennard–Jones ($N=41-2004$) and Stockmayer particles ($N=50-896$), respectively, where they calculated density profiles, surface tensions, order parameters characterizing dipole orientation, and other properties.

The work reported in this article involves a systematic MC investigation of methanol clusters, (CH$_3$OH)$_N$, $N=5-$15, 20, 30, 60, 128, and 256 and of the bulk liquid using the optimized potential for liquid simulation (OPLS) potential developed by Jorgensen.[9,48] Our main emphasis is on how the hydrogen bonding interaction which results in chainlike structures in the bulk liquid and solids will be manifested in small and large clusters. In a previous work,[35] we studied the thermodynamic and structural properties of acetonitrile clusters (CH$_3$CH)$_N$, with N in the range of 2–256. We have found that the intermolecular interactions in the small clusters ($N<12$) are dominated by dipole-dipole forces which result in antiparallel pairing of the molecular dipoles. The consequences of antiparallel dipoles are manifested in a remarkable even/odd character observed in the energies, heat capacities, and melting transitions of the small clusters. In the present study, methanol has a smaller dipole moment as compared to acetonitrile (1.7 D vs 3.9 D, respectively) but a much stronger tendency to form H-bonded clusters. Therefore, it is interesting to compare the properties of methanol clusters where hydrogen bonding plays an important role with those of the previously reported acetonitrile clusters

[a]Electronic mail: selshall@gems.vcu.edu

where dipole-dipole interaction has the major contribution to the energetics of the small clusters. Other questions addressed here include whether the molecular dipole will exhibit a preferential surface orientation in the cluster, and how the growth pattern of the clusters changes with size.

The outline of the remainder of this article is as follows. In Sec. II, we present the computational details. Section III includes the results and discussions for the bulk sample, cluster configurational energies, heat capacities, fractal dimensions, density profiles, order parameters characterizing dipole orientation, Lindemann index, and cluster stereoplots illustrating equilibrated structures. Finally, we conclude this article in Sec. IV with a summary of the salient results from this work.

II. COMPUTATIONAL ASPECTS

A. General

The cluster calculations were carried out using standard procedures including Metropolis sampling in the canonical ensemble.[49,50] Initial configurations were obtained by excising clusters from a bulk liquid sample. The maximum translation and rotation of a monomer were selected to give acceptance ratios of 25%–35%. The equilibration phases of the simulations were about 5×10^6 configurations except for the larger clusters where longer equilibration runs were made. For each N, at least two 2.5×10^7 configuration runs were made, and for $N > 15$, runs of 5×10^7 configurations were also made, mostly on account of the slower convergence of the heat capacities.

The main set of runs was made at $T = 200$ K where the clusters were liquidlike in their intermolecular motion, as indicated by the Lindemann index ($T_{mp} = 175.5$ K for bulk CH_3OH). Restraining shells were not needed as no evaporation over the duration of the reported runs was observed.

The bulk liquid was also simulated at $T = 200$ K using 128 monomers in a cubic cell and other standard procedures including periodic boundary conditions and cutoff corrections to the energy[50] (LJ, Lennard–Jones, terms only) for the potential truncation. The sample was first equilibrated at 298 K (1 atm) and then cooled to 200 K (1 atm) where it was equilibrated for 10^7 configurations in the isobaric–isothermal N-P-T ensemble. After two 4×10^6 configuration runs at 200 K (1 atm), the system density was set to the average value obtained over the two runs, the potential extended to exactly half the box length, and the system further equilibrated in the canonical NVT ensemble (N molecules in a volume V at a temperature T). The final bulk results for the energy and heat capacity were from the final 2.5×10^7 configurations run in the NVT ensemble.

B. Energies and heat capacities

The OPLS potential function[9,48] is an effective pair potential for rigid methanol monomers. This potential gives reasonably accurate results for the bulk liquid[9,48] and of the OPLS, PHH3,[12] and QPEN[51] potentials, only the OPLS

TABLE I. OPLS model parameters for methanol.

Site	q, e	σ, Å	ϵ, kcal/mol
Potential Parameters			
CH_3 (MeOH)	0.265	3.775	0.207
O	−0.700	3.070	0.170
H	0.435	0.000	0.000
Geometric Parameters:			
O–H	0.945 Å		
O–CH_3	1.430 Å		
∠H–O–CH_3	108.5 deg		

model gives satisfactory results for the second virial coefficient.[52] Each pair interaction is of the form

$$\Delta e_{ab} = \sum_i^{ona} \sum_j^{onb} \left(\frac{q_i q_j e^2}{r_{ij}} + \frac{A_{ij}}{r_{ij}^{12}} - \frac{C_{ij}}{r_{ij}^6} \right), \qquad (1)$$

where Δe_{ab} is the interaction energy between two molecules a and b, and the A and C parameters may be expressed in terms of Lennard–Jones σ's and ϵ's as $A_{ii} = 4\epsilon_i \sigma_i^{12}$ and $C_{ii} = 4\epsilon_i \sigma_i^6$. The q_i are the partial charges assigned to each site and e is the magnitude of the electron charge. Each molecule is modeled as three interaction sites (O, H, and CH_3) [i and j in Eq. (1)]. Standard bond lengths and angles based on microwave structures are assumed and the OPLS model parameters are summarized in Table I. The potential was not truncated in any of the cluster calculations.

Configurational heat capacities were calculated in the standard way from fluctuations in the cluster energy. For $N = 5$, 12, 30, and 128, where runs were also made at $T = 180$ and $T = 220$ K, C_v was also estimated from ($\Delta E/\Delta T$).

All runs were divided into segments of 10^6 configurations and standard deviations were calculated[53] using either $\sigma_1^2 = \Sigma_i^m (x_i - \bar{x})^2/m(m-1)$ or $\sigma_2^2 = \Sigma_i^m (x_i - \bar{x})^2/m$, where x_i is the average value of x over a 10^6 configuration segment of a run, $\bar{x}$ is the average of x_i over the entire run, and m is the total number of segments into which the run was divided.

C. Fractal dimension

The fractal dimension, D_f, describes the growth pattern and degree of compactness of a size series of clusters. The relation between some measure of cluster radius and the number of molecules in the cluster can be expressed as[46]

$$R_N = A N^{1/D_f}, \qquad (2)$$

where R_N is taken to be the root mean square distance between the molecules, given by[46]

$$R_N = \left\langle \left(\sum_i^{N-1} \sum_{j>i}^N \frac{r_{ij}^2}{N(N-1)} \right)^{1/2} \right\rangle \qquad (3)$$

and A is a constant. D_f was obtained by a least squares fit of $\ln N$ vs $\ln R_N$. The intermolecular distances, r_{ij}, were taken as the separations of the molecular centers-of-mass.

D. Density profiles

A density profile gives the average number density as a function of distance from the center of the cluster. Density profiles were calculated for each potential site in the molecu-
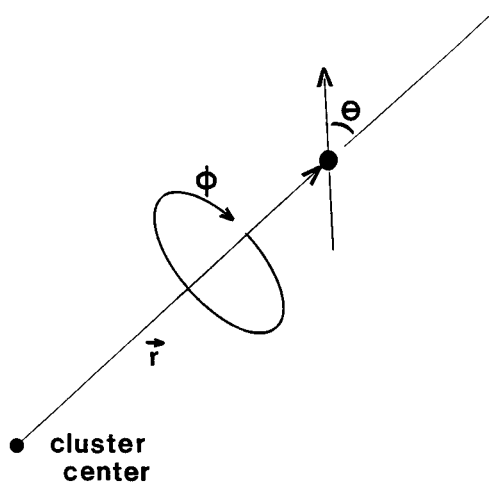
FIG. 1. Geometry for the order parameter calculation.

lar model where the cluster center was taken as the oxygen atom nearest the cluster center-of-mass. A density profile was also calculated for the ''effective dipoles'' (for calculation of the dipole order parameters) where the center of the cluster was taken to be the dipole nearest the center-of-mass. As the effective dipole is located close to the oxygen atom, the oxygen and dipole density profiles are very similar. The width of each spherical bin was 0.05 Å and the calculation was performed every 500 configurations except for the $N=256$ system where it was done every 2500 configurations.

E. Order parameters

For molecular clusters, the density orientational profile $\rho(r,\theta)$ can be expanded in terms of Legendre polynomials $P_n(\cos \theta)$ as[41]

$$\rho(r,\theta)=\sum_n \hat{\rho}_n(r)P_n(\cos \theta), \tag{4}$$

where $\hat{\rho}_n(r)$ is an order parameter and θ is the angle between the dipole vector (or a bond vector) of a molecule and its radial position vector. We define θ and ϕ as in the spherical coordinate system taking the radial position vector of each dipole to be the z axis of the spherical system, as shown in Fig. 1. The density $\rho(r,\theta)$ is given by

$$\rho(r,\theta)=\int_0^{2\pi} d\phi\, \rho(r,\theta,\phi), \tag{5}$$

and $\rho(r)$ can be obtained by integrating this over θ,

$$\rho(r)=\int_0^{\pi} \rho(r,\theta)\sin \theta d\theta. \tag{6}$$
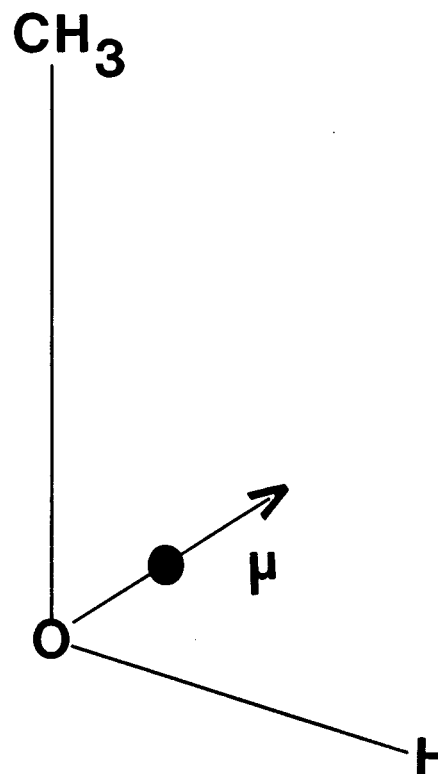
We define for each r

FIG. 2. Geometry for the effective dipole of methanol.

$$\langle P_n(\cos \theta)\rangle=\frac{\int_0^{\pi} \sin \theta d\theta \rho(r,\theta)P_n(\cos \theta)}{\int_0^{\pi} \sin \theta d\theta \rho(r,\theta)}. \tag{7}$$

Multiplying both sides of Eq. (5) by $P_n (\cos \theta)$ and integrating over θ gives

$$\hat{\rho}_n(r)=\frac{(2n+1)}{2}\int_0^{\pi} \sin \theta d\theta \rho(r,\theta)P_n(\cos \theta) \tag{8}$$

and using Eq. (7) we get

$$\hat{\rho}_n(r)=\frac{(2n+1)}{2}\rho(r)\langle P_n(\cos \theta)\rangle. \tag{9}$$

These order parameters are a measure of dipole (or bond vector) orientation relative to their radial position vectors. Near the surface of spherical clusters this is equivalent to their orientation relative to the surface normal.

For each methanol molecule, an effective dipole vector is assigned as shown in Fig. 2. The length of this vector is determined by $\mu=qd$ where μ is the magnitude of the dipole moment and q is the magnitude of the charge on the site carrying the negative charge and d is the length of the dipole. The OPLS potential gives a dipole moment of 2.22 D for CH_3OH (1.7 expt.) as it is an effective pair potential. The orientation of the MeOH dipole vector is given by the vector sum of the dipoles along the O–H and O–Me bonds as determined by the partial charges on the molecules. This effec-

tive dipole vector approximately bisects the H–O–Me bond angle ($\angle \mu - O - CH_3 = 57.5°$) and is centered about 0.33 Å from the oxygen. The values of $\langle \cos^n \theta \rangle$ for $n = 1-4$ were calculated as a function of radius, and from these the $\langle P_n(\cos \theta) \rangle$ were calculated.[54] The order parameters were then calculated for each r using Eq. (9).

Similar calculations were also carried out to obtain information on the orientation of the O→H and O→CH_3 bond vectors where the oxygen nearest the center-of-mass was taken as the origin. These order parameters are denoted $\hat{\rho}_n$ (O–H) and $\hat{\rho}_n$ (O–CH_3), respectively, and the corresponding notation for the dipole order parameters is $\hat{\rho}_n(\mu)$. The geometry was the same as that used for the dipole calculation where the dipole vector was replaced by the appropriate bond vector. All other details were completely analogous to the dipole calculation and a density of bond vectors at a radius r was also obtained as needed for these order parameters.[54] All order parameter calculations were performed every 500 configurations except for the $N = 256$ system where it was done every 2500 configurations.

F. The Lindemann index

The Lindemann index, δ, has been used for both atomic[27] and molecular[29–37] clusters for the study of melting and coexistence phenomena, and is defined as the average root-mean-square fluctuation in intermolecular separation which is given by[24,37]

$$\delta = \frac{2}{N(N-1)} \sum_{i}^{N-1} \sum_{j>1}^{N} \frac{(\langle r_{ij}^2 \rangle - \langle r_{ij} \rangle^2)^{1/2}}{\langle r_{ij} \rangle}, \quad (10)$$

where the r_{ij} are the intersite separation distances. This calculation was performed for the O–O, H–H, and CH_3–CH_3 motions for each cluster except for $[CH_3OH]_{256}$.

For atomic systems, Lindemann's criteria for melting states that a value of $\delta > 0.1$ indicates a liquidlike cluster and a value of $\delta < 0.1$ indicates a solidlike form. As discussed by Bartell *et al.*,[30] the r_{ij} values in polyatomic clusters are longer than the true atom-atom contact distances. Also, small molecules are typically treated as rigid particles in most MC simulations and thus intramolecular vibrations are neglected. These effects lower the threshold value of δ for molecular clusters from the value of 0.1 at which atomic systems are considered to melt.

As our initial reason for calculating δ was to ensure that the clusters were liquidlike at the simulation temperatures, the averaging in Eq. (10) was, for simplicity, over all r_{ij} in the cluster. Thus, for clusters with $N > 20$, we have obtained only a lower bound on δ. This was sufficient to ensure the nonrigidity of the clusters.

III. RESULTS AND DISCUSSION

A. Bulk sample

The two bulk runs in the N-P-T ensemble resulted in an average density of 0.851 ± 0.003 g/cm^3. (The same value obtained in Ref. 55 using 256 monomers and the MD method.) At this density in the NVT ensemble, the average configura-
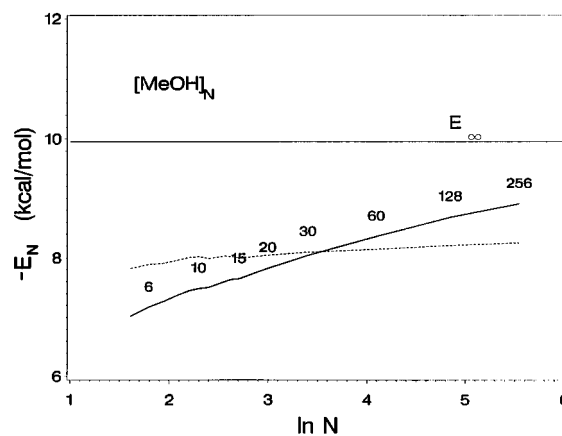

FIG. 3. Average configurational energy per molecule in a cluster of size N for $[CH_3OH]_N$ (solid line). Dashed line is the Coulomb potential terms only. The bulk value is shown as a horizontal line.

tional energy per molecule was 9.944 ± 0.005 kcal/mol and the average configurational heat capacity per molecule was 7.8 ± 0.2 cal/mol K.

B. Cluster energies and heat capacities

Figure 3 shows that the OPLS cluster energy per molecule at 200 K is already at 70% of the bulk at $N = 5$, rising to 90% at $N = 256$. The standard deviations for the multiple runs are less than the thickness of the lines. The energy arising from the Coulomb type terms of the potential energy (shown in Fig. 3) indicates that at small sizes the entire cohesive force arises from these terms. Only for $N > 30$, do the LJ terms become net attractive. In simulations of the bulk liquid at 298 K, Jorgensen[9] observed that the LJ terms are also net repulsive when only the energy arising from hydrogen bonding is considered. That the energy of $[CH_3OH]_{256}$ is only 10% less than that of the bulk liquid indicates the dominance of short range interactions, i.e., hydrogen bonds, in the total bulk energy. In general, one might expect cluster energies to differ from the bulk less in systems dominated by short range interactions. Also, the average number of hydrogen bonds per molecule in the bulk liquid is about 1.8,[9] and thus for the smaller clusters where each molecules has 2 H-bonds, it is not surprising that they have 70% or more of the energy per molecule of the bulk.

For acetonitrile clusters[35] at 120 K, the Coulomb terms contribute about 50% of the total energy for the small clusters ($N < 12$). The methanol clusters show a significant difference where, as shown in Fig. 3, all the binding energies for the smaller clusters ($N < 30$) are entirely due to the Coulomb terms. This is due to the short range H-bonding interactions in methanol clusters which result in shorter distances between the molecules such that the LJ terms become net repulsive. Another difference between the energetics of acetonitrile and methanol clusters is the absence of the even/odd character in methanol clusters. This feature was observed in the energy per molecule in acetonitrile clusters and
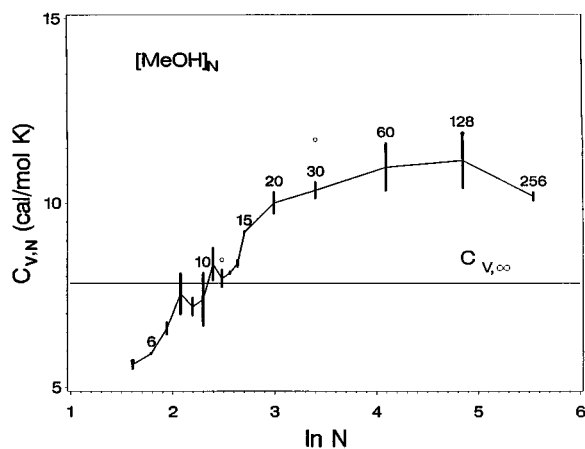
FIG. 4. Average configurational heat capacity per molecule in a cluster of size N for $[CH_3OH]_N$ (solid line). The bulk value is shown as a horizontal line. Circles represent heat capacities calculated from $(\Delta E/\Delta T)$ for $N=5, 12, 30,$ and 128.
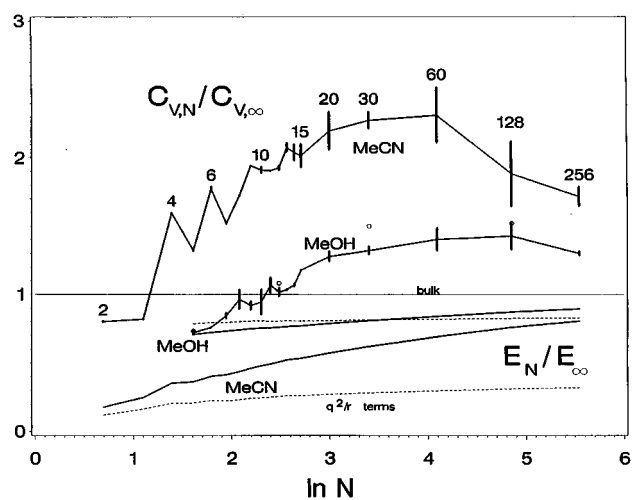

FIG. 5. Ratios of the cluster energies and heat capacities per molecule to the values obtained from simulations of the bulk at the same temperature, 120 K for acetonitrile and 200 K for methanol.

was attributed to the antiparallel pairing of the molecular dipoles.

The cluster heat capacities in the $N=5$–256 range are plotted as a function of N at 200 K (where all the clusters are liquidlike except for $N=256$) in Fig. 4 along with the corresponding bulk value. The heat capacities rise from below the bulk value at small N, reach a maximum between $N=60$ and $N=128$, and then fall off, suggesting convergence to the bulk from above. A similar trend has also been observed for acetonitrile clusters in this size range[35] and this trend is probably a rather general result. The rapid increase in heat capacity with increasing N at smaller sizes results from the rapid increase in cluster energy per molecule and the rapid increase in the number of available isomers which results in greater frequency of isomerization and consequently, greater fluctuations in the energy. At larger N, the heat capacities tend to decrease since the rate of increase in the energy per molecule decreases and also due to the $N^{-1/2}$ dependence of fluctuations ($N^{-1/2}$ is twice as large for $N=60$ as for $N=256$). The net result is an interior maximum in the C_v vs N plot which appears around $N=60$–128 as indicated in Fig. 4. Hoare and Pal[56] have observed an interior maximum in the calculated vibrational heat capacities of small rigid argon clusters within the harmonic-oscillator approximation. With this model, the vibrations are actually interparticle motions determined by the interatomic (Lennard–Jones) potential, and thus the analogy with intermolecular configurational heat capacities may be reasonable.

For $N=5, 12, 30,$ and 128, the heat capacities as calculated from the temperature dependence of the energy are also shown in Fig. 4 (open circles). They are reasonably close to the heat capacities calculated from the fluctuations formula with the exception of $N=30$, where the value from $(\Delta E/\Delta T)_v$ is the somewhat higher than the fluctuation result. The overall shape of the size dependence of $(\Delta E/\Delta T)_v$ is consistent with the fluctuation results. Note that this calculation involves a relatively small difference of two larger terms

(each accurate to no more than 3 significant figures) and ΔT was only 40 K.

It is interesting to compare the energetics and heat capacities of methanol and acetonitrile clusters. In Fig. 5, we illustrate such comparisons by plotting the ratios of the cluster to bulk values for the energies and heat capacities for both $(CH_3OH)_N$ and $(CH_3CN)_N$ vs $\ln N$. It should be noted that the simulation temperatures for methanol and acetonitrile were 200 and 120 K, respectively. At these temperatures, the clusters with $N<128$ were clearly liquidlike in their intermolecular motion as indicated by their Lindemann indices. The most significant feature in Fig. 5 is that for both the energies and heat capacities, the results for acetonitrile clusters differ from the bulk values substantially more than those of methanol clusters. In other words, there is a much stronger apparent ''size effect'' for the acetonitrile system. Part of this pronounced difference is probably due to the difference in the simulation temperatures of the two systems. However, if we were to increase the temperature for acetonitrile from 120 K to the same reduced temperature ($T_r=T/T_c$) as that of methanol at 200 K ($T_r=0.39$), the corresponding temperature for acetonitrile would be 213 K and we would still see that the energies of acetonitrile clusters differ from the bulk value substantially more than those of methanol clusters at the same reduced temperature. The difference between the cluster and bulk energies is probably related to the nature of intermolecular interactions within the clusters and in the bulk liquid. Therefore, it appears that molecular clusters dominated by H-bonding interactions would exhibit properties very similar to the bulk liquid.

C. Fractal dimension

D_f was found to be 2.89 when all sizes are included in the regression. When only the $N>13$ clusters were included, the plot is more linear and gives $D_r=3.15$. Figure 6 shows a plot of $\ln R_N$ vs $\ln N$ and the pronounced change of slope
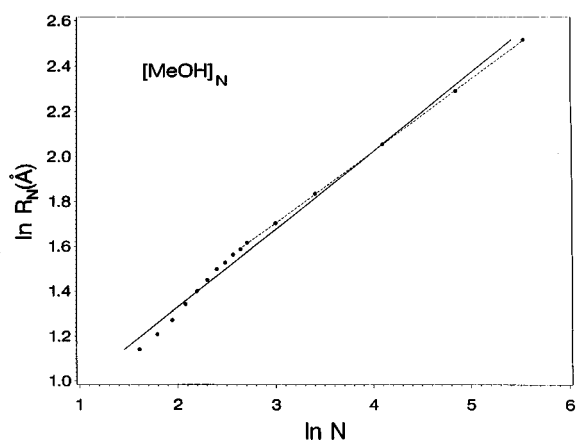
FIG. 6. $\ln R_N$ vs $\ln N$ for $[CH_3OH]_N$. The lines are least squares fits (solid—$N=5$–256, dotted—$N=14$–256).

around $N=14$ correlates well with the cluster structures shown in the stereoplots (Figs. 13–15) and to be discussed in Sec. III G.

For a series of spheres of different sizes having the same density, one obtains a fractal dimension of 3, the Euclidean dimension. D_f values greater than 3 can be interpreted as a result of the clusters becoming more compact with increasing N, and especially in this case with the cyclic semiplanar structures for $N<15$. We previously reported a D_f value 3.10 for acetonitrile clusters in the size range $N=2$–256 ($D_f=3.03$ for $N=20$–256 only).[35,54] Tight-binding calculations on small sodium clusters[57] ($N=2$–34) yielded a fractal dimension of about 3.1 for the minimum energy ($T=0$ K) structures. It appears that a fractal dimension greater than 3 would result if the smaller clusters were nonspherical, and values around 3 are probably to be expected for isolated clusters cold enough to exist without restraining shells to prevent evaporative loss.

The fractal dimension for Lennard–Jones clusters in their vapor has been found by Gregory[46] and Heyes[47] to be in the range of $D_f=2.3$–2.5. For Stockmayer molecules, Schug[58] has obtained a value of about 2.5. Our result for the isolated methanol clusters is significantly higher than those of these cluster-vapor systems, probably due to the lower temperatures of this work, as judged by the lower vapor pressures of these (isolated) methanol clusters.

D. Density profiles

The oxygen (O–O) and the hydrogen (H–H) density profiles for $N=15$, 20, 30, 60, 128, and 256 at 200 K are shown in Fig. 7 for runs of 5.0×10^7 configurations, along with the average density of the bulk liquid at the same temperature. The dominant feature in the (O–O) density profiles is an extremely sharp peak due to the first H-bond accepting neighbors which can be seen in Fig. 7(a) at separation of about 2.8 Å. For all sizes ($N=5$–256), integration of the first peak in the oxygen profile gives two, as two molecules are hydrogen bonded to the central molecule, and integration of the first peak in the hydrogen profile gives one, as the central
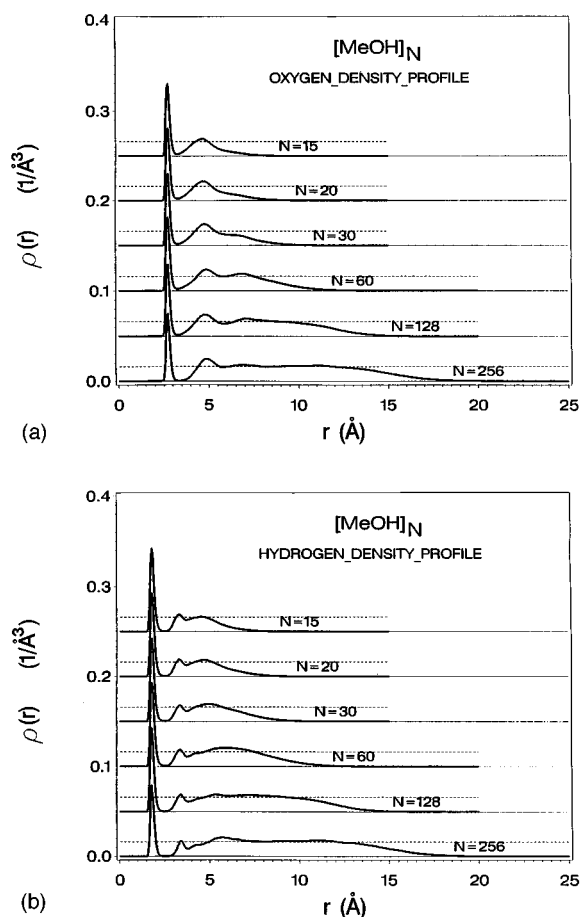

FIG. 7. (a) Oxygen (O–O) density profiles for $[CH_3OH]_N$, $N=15$, 20, 30, 60, 128, and 256. Dotted horizontal lines represent the average bulk density. (b) Hydrogen density profiles for $[MeOH]_N$, $N=15$, 20, 30, 60, 128, and 256. Dotted horizontal lines represent the average bulk density.

molecule provides one of the hydrogens (and is thus not counted) for its two hydrogen bonds. As expected, these profiles at 200 K are very similar to the radial distribution functions [$g(r)$'s] of the bulk liquid at 298 K, although the minimum following the first peak in the profiles of the larger clusters goes to zero, unlike the bulk $g(r)$, and the larger clusters show slightly more structure than the bulk. In fact, the minimum after the first peak slowly drops to zero as the cluster size increases, and the second peak decreases slightly in width. These features, although weak, indicate that the larger clusters are slightly more rigid than the smaller ones in the size range $N=15$–256. Sindzingre and Klein[18] have observed a similar trend for bulk methanol with decreasing temperature rather than increasing system size. Given that cluster melting points generally decrease with decreasing cluster size, one would expect that at some temperatures small clusters would be liquidlike with rigidity increasing with size, and sufficiently large clusters would be solidlike.

Note that the density of the larger clusters falls off significantly only at rather large radii. This is in contrast to the results for higher temperature Lennard–Jones[42,46] and Stockmayer[41] clusters where the density profiles show significant decreases at much smaller radii (relative to the over-
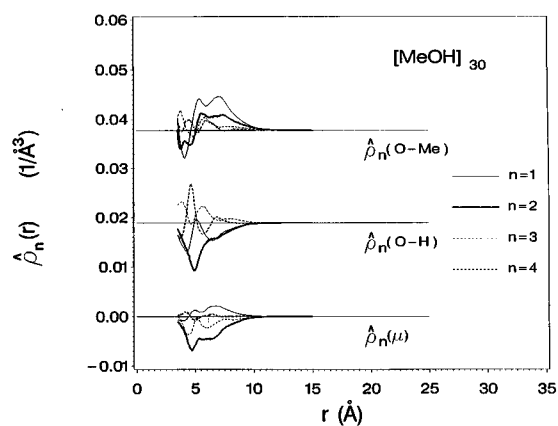
FIG. 8. Order parameters for $[CH_3OH]_{30}$.
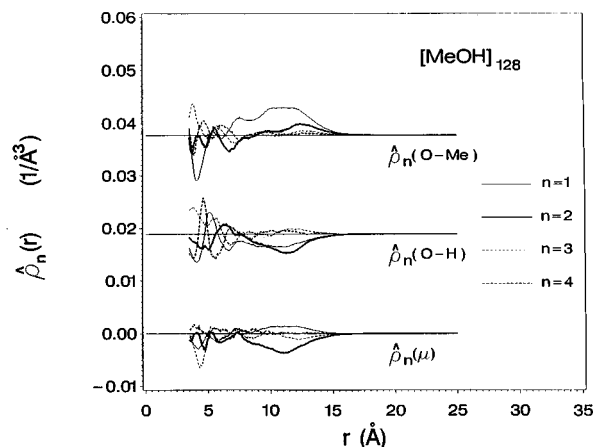
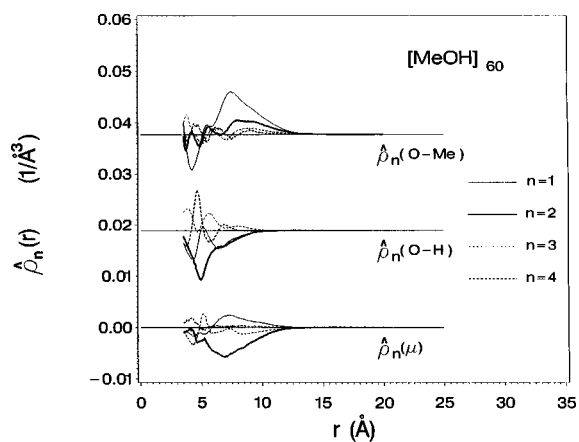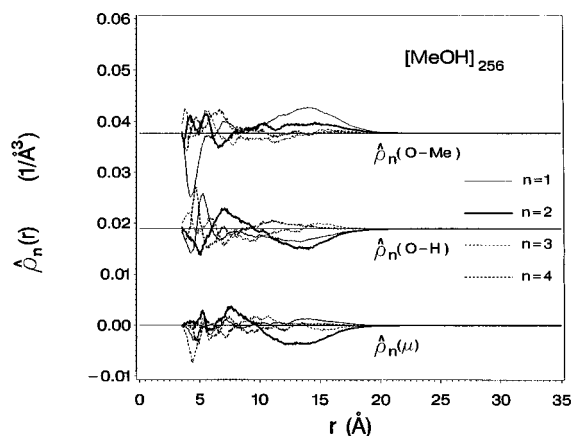FIG. 10. Order parameters for $[CH_3OH]_{128}$.

all cluster radius). This suggests that the higher temperature clusters possess a wider interfacial region than the cooler ones. This has been observed in MD simulations of the planar liquid-vapor interface for methanol.[59] That the cluster densities only fall off at rather large radii also correlates with the relatively large fractal dimension obtained for $[CH_3OH]_N$. Comparison of the cluster densities at large radii for $[CH_3OH]_{128}$ and $[CH_3OH]_{256}$ with the average density of the bulk liquid at the same temperature suggests that the overall cluster density is rather well represented by the bulk value.

E. Order parameters

These parameters are most meaningful for the larger clusters. The results for all three sets of order parameters are shown in Figs. 8–11 for the $N=30$, 60, 128, and 256 clusters, respectively, for runs of 5.0×10^7 configurations. The significantly negative values for $\hat{\rho}_2(\mu)$ at large radii indicate a net tendency for the effective dipoles to lie perpendicular to the radial position vector and therefore (for a spherical cluster) parallel to the surface of the cluster. The small positive $\hat{\rho}_1(\mu)$ at larger radii indicates a slight preference for an out-

ward rather than inward orientation. The negative values for $\hat{\rho}_2$ (O–H) also indicate a net tendency for these bond vectors to lie somewhat parallel to the surface at large r, and here the small negative $\hat{\rho}_1$(O–H) indicates a slight preference for an inward rather than outward orientation. The pronounced positive $\hat{\rho}_1$(O–CH$_3$) at large r indicates a net tendency for an outward orientation of the O→Me bond vectors near the surface of the cluster. All of this taken together is consistent with the orientation of the effective dipole in the molecular model shown in Fig. 2. Comparison of these parameters for all four sizes suggests that the bulk surface orientation effect extends well into the cluster regime within the size range $N=30$–256. We have also observed this tendency for dipole orientation parallel to the surface in acetonitrile clusters in the size range $N=30$–256.[35]

Mitsuhiro et al.[59] have studied the planar liquid-vapor interface of methanol at several temperatures with MD simulations and have observed a very similar surface ordering with the methyl groups outward and the effective dipoles parallel to the liquid surface. This is explained as a result of the hydrophobic nature of the methyl groups and the maximization of hydrogen bonding. In contrast to water, the

FIG. 9. Order parameters for $[CH_3OH]_{60}$.
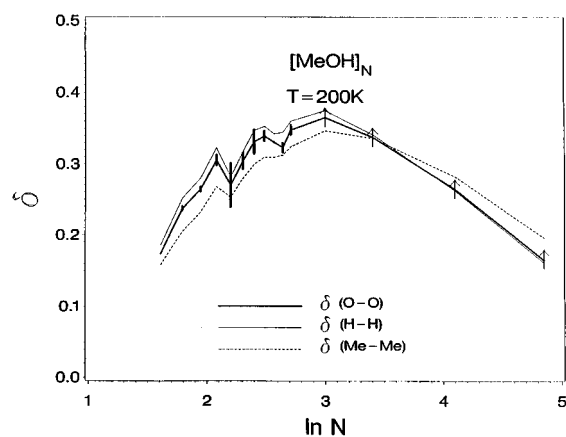

FIG. 11. Order parameters for $[CH_3OH]_{256}$.

FIG. 12. The Lindemann index vs N for $[CH_3OH]_N$, $N = 5-128$, at $T = 200$ K for the H–H, O–O, and CH_3–CH_3 site separations. Up arrows indicate values that are lower limits.

FIG. 14. Stereoplots for $[CH_3OH]_N$, $N = 9-12$ at $T = 200$ K. Filled circles represents the CH_3 groups and dark circles represent the O atoms.

methanol molecule has a hydrophobic and a hydrophilic end which results in stronger orientational tendency than water. They also note that the probable surface orientation of water is the one where the effective dipole (C_2 axis) is parallel to the liquid surface. In their MD simulations of Stockmayer drops (in equilibrium with vapor), Shreve *et al.*[41] observed a similar tendency for the surface dipoles to align parallel to the cluster surface for liquid drops containing 260 and 896 particles, although for a smaller droplet containing only 50 molecules this effect was absent.

These results suggest that a parallel-to-surface dipole orientation is probably a general feature of liquidlike clusters of polar molecules (of sufficient size).

F. The Lindemann index

Figure 12 shows the Lindemann index for $[CH_3OH]_N$ at 200 K where representative error bars (σ_2's) are attached for $N < 20$. For $N < 20$, the plotted results are the averages over
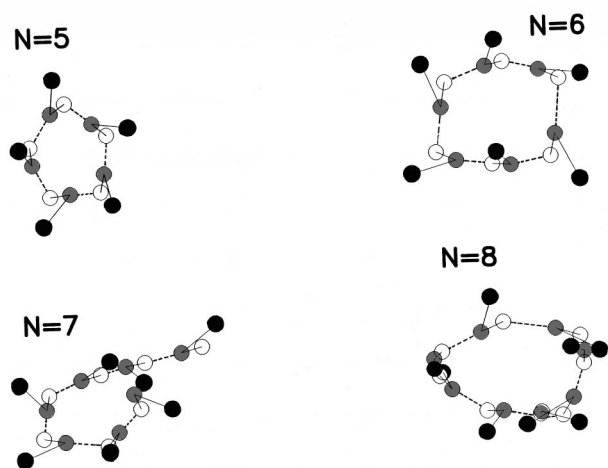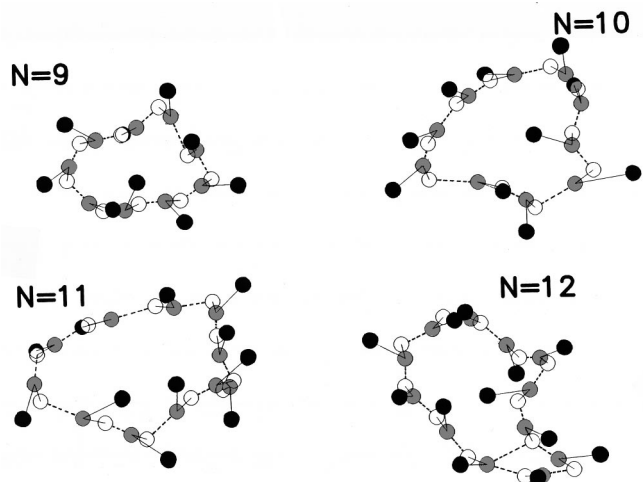
the multiple runs and for $N > 20$ the results are from the 5×10^7 configuration runs only. The arrows for $N > 20$ indicate that these values are to be taken as lower limits for the actual values, as discussed above. These clusters are clearly liquidlike in their intermolecular motion as $\delta > 0.1$ for all of these clusters. The dip in the index for $[CH_3OH]_9$ could be interpreted as an indication of a relatively more rigid cluster with some difficulty for isomerization relative to the neighboring clusters.

G. Cluster stereoplots

For the smaller ($N < 30$) clusters, two or more equilibrated configurations were arbitrarily selected and stereo plotted, as well as a single configuration for the larger clusters. For the smaller clusters, the features were the same in each of the examined snapshots.

Figures 13–16 illustrate the growth pattern of methanol clusters at $T = 200$ K, with the transition from semiplanar monoclyclic structures in the $N = 5-12$ size range, to bi- and
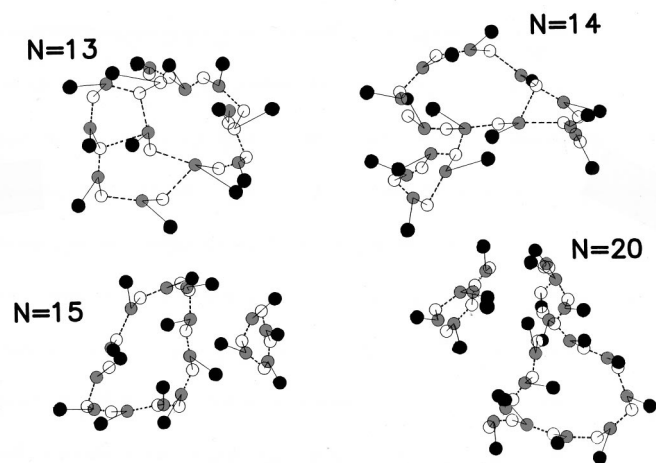

FIG. 13. Stereoplots for $[CH_3OH]_N$, $N = 5-8$ at $T = 200$ K. Filled circles represent the CH_3 groups and dark circles represent the O atoms.

FIG. 15. Stereoplots for $[CH_3OH]_N$, $N = 13-20$ at $T = 200$ K. Filled circles represent the CH_3 groups and dark circles represent the O atoms.
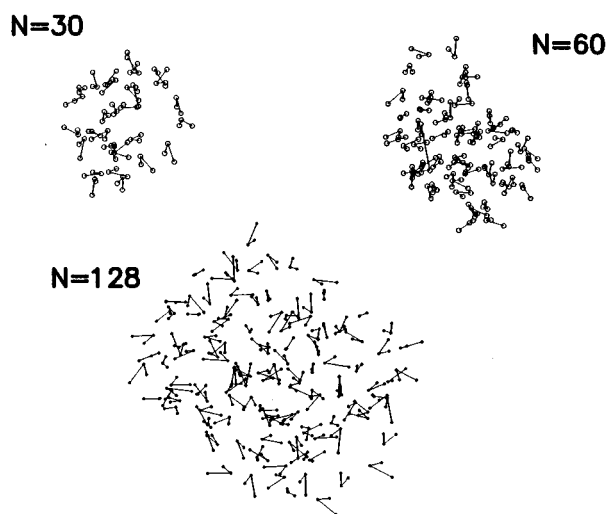
FIG. 16. Stereoplots for $[CH_3OH]_N$, $N=30$–128 at $T=200$ K. Filled circles represents the CH_3 groups and dark circles represent the O atoms.

polycyclic structures in the $N=13$–20 range, and then to more spherical ''microdropletlike'' structures in the $N=30$–256 size range. Figure 16 indicates that clusters as large as 30 and 60 molecules may have cavities and are not especially spherical. In Fig. 15, cyclic tetramers can be identified in the $N=15$ and $N=20$ snapshots, which is not surprising considering the special stability of the cyclic tetramer.[60]

As noted below, this growth pattern correlates well with the marked change of slope in $\ln N$ vs $\ln R_N$ shown in Fig. 6 near $N=14$, i.e., it is around $N=13$–15 that the clusters cease to grow by enlarging a primary semiplanar ring and begin a transition to more compact 3-dimensional growth.

Minimum energy structures for $[CH_3OH]_N$, $N=2$–6, 9, and 10 have been obtained from both empirical potentials[52,61–64] and *ab initio* calculations.[60,65] Although the binding energies differ, the minimum energy geometries were always cyclic. Molecular beam electric deflection experiments[66] have indicated an upper limit for the dipole moments of small ($N=3$–4) methanol clusters of about 0.3 D, and this has been interpreted as evidence of cyclic semiplanar structures.

IV. SUMMARY AND CONCLUSIONS

In summary, we note the following features of isolated methanol clusters.

(1) The attractive interactions in small methanol clusters ($N<30$) are entirely due to the Coulomb potential terms which are responsible for the strong tendency to form H-bonding structures. Cyclic structures have been observed for small clusters ($N=5$–12). The observation of ringlike structures for clusters as large as 12–15 molecules at a temperature 25 K above the freezing point of the bulk liquid (and with a very liquidlike Lindemann index) is striking. This may suggest that the ringlike structures of the finite clusters could evolve into the chainlike polymeric units observed in the bulk liquid at lower temperatures.

(2) Although the planar cyclic hexamer is clearly evident in our structural data for $(CH_3OH)_6$, no evidence to support the formation of multiple hexagonal rings has been found for larger clusters. Only cyclic tetramers could be identified within the bi- and polycyclic structures in the intermediate size range $N=12$–20. In larger clusters, quasispherical structures are not reached until about $N>100$ and they show no apparent formation of local cyclic hexagonal clusters as suggested recently by Sarkar and Joarder in their study of bulk liquid methanol.[20]

(3) The heat capacities as a function of N possess an interior maximum as a result of the rapid increase in energy and number of isomers at smaller sizes and the decrease in fluctuations at larger sizes.

(4) At $T=200$ K, the density profiles fall off at relatively larger radii than those of higher temperature clusters formed in equilibrium with their vapors. This is also reflected in the larger fractal dimensions observed for the methanol clusters. The average density of the larger clusters is fairly well represented by the bulk value.

(5) The larger clusters ($N>20$) show a net tendency for the dipole moment vectors to lie somewhat flat on the cluster surface, as previously observed for clusters of Stockmayer molecules and also for acetonitrile clusters.

(6) The observed trends in heat capacities, density profiles, and dipole alignments parallel to the cluster surface are likely to be general features of clusters of polar molecules.

ACKNOWLEDGMENTS

[1] *The Hydrogen Bond*, edited by P. Schuster, G. Zundel, and C. Sanfordy (North Holland, Amsterdam, 1976), Vol. 1–3.

[2] C. Reichardt, *Solvents and Solvent Effects in Organic Chemistry*, 2nd ed. (VCH, F. R. Germany, 1988).

[3] *Organic Liquids: Structure, Dynamics, and Chemical Properties*, edited by A. D. Buckingham, E. Lippert, and S. Bratos (Wiley, New York, 1978).

[4] J. N. Israelachvili, *Intermolecular and Surface Forces*, 2nd ed. (Academic, London, 1992).

[5] A. H. Narten and A. Habenschuss, J. Chem. Phys. **80**, 3387 (1984).

[6] D. C. Steytler, J. C. Dore, and D. C. Montague, J. Non-Cryst. Solids **74**, 303 (1985).

[7] W. L. Jorgensen, J. Am. Chem. Soc. **102**, 543 (1980); **103**, 341 (1981).

[8] J. K. Vij, C. J. Reid, and M. W. Evans, Mol. Phys. **50**, 935 (1983).

[9] W. L. Jorgensen, J. Phys. Chem. **90**, 1276 (1986).

[10] M. Haughney, M. Ferrario, and I. R. McDonald, Mol. Phys. **58**, 849 (1986).

[11] M. Haughney, M. Ferrario, and I. R. McDonald, J. Phys. Chem. **91**, 4934 (1987).

[12] G. Palinkas, E. Hawlicka, and K. Heinzinger, J. Phys. Chem. **91**, 4334 (1987).

[13] E. Hawlicka, G. Palinkas, and K. Heinzinger, Chem. Phys. Lett. **154**, 225 (1989).

[14] F. J. Bermejo, F. Batallan, E. Enciso, R. White, A. J. Dianoux, and W. S. Howells, J. Phys. Condens. Matter **2**, 1301 (1990).

[15] M. Matsumoto and K. E. Gubbins, J. Chem. Phys. **93**, 1981 (1990).

[16] T. Fonseca and B. M. Ladanyi, J. Chem. Phys. **93**, 8148 (1990).

[17] J. Alonso, F. J. Bermejo, M. Garcia-Hernandez, J. L. Martinez, and W. S. Howells, J. Mol. Struct. **250**, 147 (1991).

[18] P. Sindzingre and M. L. Klein, J. Chem. Phys. **96**, 4681 (1992).

[19] I. M. Svishchev and P. G. Kusalik, J. Chem. Phys. **100**, 5165 (1994).

[20] S. Sarkar and R. N. Joarder, J. Chem. Phys. **99**, 2032 (1993).

[21] R. S. Berry, T. L. Beck, H. L. Davies, and J. Jellinek, Adv. Chem. Phys. **70**, 74 (1988).

[22] J. Jortner, D. Scharf, and U. Landman, in *Elemental and Molecular Clusters*, edited by G. Benedek, T. P. Martin, and G. Pacchioni (Springer, Berlin, 1988).

[23] R. S. Berry, in *The Chemical Physics of Atomic and Molecular Clusters*, edited by G. Scholes (North-Holland, Amsterdam, 1990).

[24] J. Jellinek, T. L. Beck, and R. S. Berry, J. Chem. Phys. **84**, 2783 (1986).

[25] D. J. Wales and R. S. Berry, J. Chem. Phys. **92**, 4283 (1990).

[26] H. L. Davis, J. Jellinek, and R. S. Berry, J. Chem. Phys. **86**, 6456 (1987).

[27] T. L. Beck, J. Jellinek, and R. S. Berry, J. Chem. Phys. **87**, 545 (1987).

[28] G. Del Mistro and A. J. Stace, Chem. Phys. Lett. **171**, 381 (1990).

[29] F. J. Dulles and L. S. Bartell, J. Phys. Chem. **99**, 17 100 (1995).

[30] L. S. Bartell, F. J. Dulles, and B. Chuko, J. Phys. Chem. **95**, 6481 (1991).

[31] L. S. Bartell and J. Chen, J. Phys. Chem. **99**, 12 444 (1995).

[32] R. D. Etters, K. Flurchick, R. P. Pan, and V. Chandrasekharan, J. Chem. Phys. **75**, 929 (1981).

[33] L. S. Bartell and S. Xu, J. Phys. Chem. **99**, 10 446 (1995).

[34] A. S. Al-Mubarak, G. Del Mistro, P. G. Lethbridge, N. Y. Abdul-Sattar, and A. J. Stace, Discuss. Faraday Soc. **86**, 209 (1988).

[35] D. Wright and M. S. El-Shall, J. Chem. Phys. **100**, 3791 (1994).

[36] G. Del Mistro and A. J. Stace, J. Chem. Phys. **99**, 4656 (1993).

[37] D. J. Wales and I. Ohmine, J. Chem. Phys. **98**, 7245 (1993).

[38] D. J. Wales and I. Ohmine, J. Chem. Phys. **98**, 7257 (1993).

[39] H. Sun, R. O. Watts, and U. Buck, J. Chem. Phys. **96**, 1810 (1992).

[40] G. Cardini, V. Schettino, and M. L. Klein, J. Chem. Phys. **90**, 4441 (1988).

[41] A. P. Shreve, J. P. R. B. Walton, and K. E. Gubbins, J. Chem. Phys. **85**, 2178 (1986).

[42] S. M. Thompson, K. E. Gubbins, J. P. R. B. Walton, R. A. R. Chandry, and J. S. Rowlinson, J. Chem. Phys. **81**, 530 (1984).

[43] J. G. Powles, R. F. Fowler, and W. A. B. Evans, Chem. Phys. Lett. **107**, 280 (1984).

[44] J. G. Powles, R. F. Fowler, and W. A. B. Evans, Chem. Phys. Lett. **96**, 289 (1983).

[45] J. G. Powles, R. F. Fowler, and W. A. B. Evans, Phys. Lett. A **98**, 421 (1983).

[46] V. P. Gregory and J. C. Schug, Mol. Phys. **78**, 407 (1993).

[47] D. M. heyes and J. R. Melrose, Mol. Phys. **66**, 1057 (1989).

[48] W. L. Jorgensen, J. D. Madura, and C. J. Swenson, J. Am. Chem. Soc. **106**, 6638 (1984).

[49] N. Metropolis, A. W. Rosenbluth, M. N. Rosenbluth, A. H. Teller, and E. Teller, J. Chem. Phys. **21**, 1087 (1953).

[50] M. P. Allen and D. J. Tildesley, *Computer Simulation of Liquids* (Oxford University Press, Oxford, 1991).

[51] F. T. Marchese, P. K. Mehrota, and D. L. Beveridge, J. Phys. Chem. **82**, 2497 (1978).

[52] U. Buck and B. Schmidt, J. Chem. Phys. **98**, 9410 (1993).

[53] W. L. Jorgensen, Chem. Phys. Lett. **92**, 405 (1982).

[54] D. Wright, Ph.D. dissertation, Virginia Commonwealth University, Richmond, VA (1993).

[55] M. Matsumoto and K. E. Gubbins, J. Chem. Phys. **93**, 1981 (1990).

[56] M. R. Hoare and P. Pal, Mol. Phys. Adv. Phys. **24**, 645 (1975).

[57] R. Poteau and F. Spiegelmann, J. Chem. Phys. **98**, 6540 (1993).

[58] J. C. Schug (private communication).

[59] M. Mitsuhiro and Y. Kataoka, J. Chem. Phys. **90**, 2398 (1989).

[60] L. A. Curtiss, J. Chem. Phys. **67**, 1144 (1977).

[61] U. Buck, X. J. Gu, Ch. Lauenstein, and A. Rudolph, J. Chem. Phys. **92**, 6017 (1990).

[62] T. P. Martin, T. Bergmann, and B. Wassermann, in *Large Finite Systems*, edited by J. Jortner and B. Pullmann (Reidel, Dordrecht, 1987).

[63] G. Brink and L. Glasser, J. Comput. Chem. **2**, 14 (1981).

[64] U. Buck, Ber. Bunsenges. Phys. Chem. **96**, 1275 (1992).

[65] E. H. S. Anwander, M. M. Probst, and B. M. Rode, Chem. Phys. **166**, 341 (1992).

[66] J. A. Odutola, R. Viswanathan, and T. R. Dyke, J. Am. Chem. Soc. **101**, 4787 (1979).